

Supplemental Table S1. The list of peptides identified in TAP-WPP1 LC/MS/MS analysis, corresponding to HSC70.

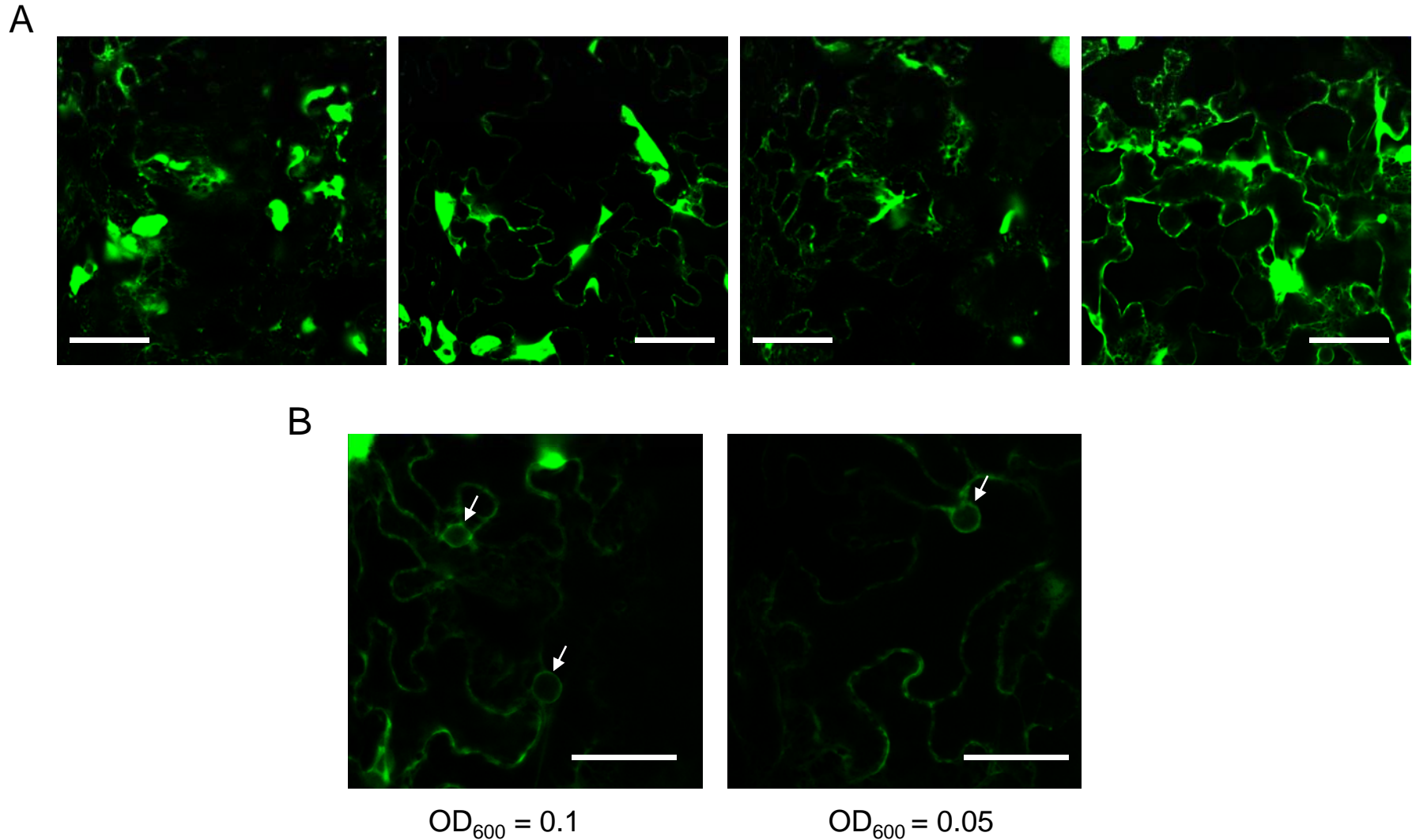
peptide	MH+	charge	XCorr score	Delta Cn score	Protein ID
KNAVVTVPAYFNDSQRQ	1680.83	2	2.22	0.37	At1g56410 (HSP70T-1) At1g16030 (HSP70B) At3g12580 (HSP70) At5g02490 (HSC70-2) At3g09440 (HSC70-3) At5g02500 (HSC70-1)
RIINEPTAAAIAYGLDKKG	1787.99	2	3.18	0.58	At5g42020 (BiP) At1g56410 (HSP70T-1) At1g16030 (HSP70B) At3g12580 (HSP70) At5g28540 (BiP-1) At5g02490 (HSC70-2) At3g09440 (HSC70-3) At5g02500 (HSC70-1)
KEQVFSTYSDNQPGVLIQVYEGERA	2658.27	2	4.23	0.59	At3g09440 (HSC70-3) At5g02500 (HSC70-1)
KSINPDEAVAYGAAVQGAILS GEGNEKV	2560.25	2	6.27	0.47	At5g02500 (HSC70-1)

Predicted mass (MH+) and charge values, as well as confidence parameters (Xcorr and Delta Cn) are indicated for each peptide. Protein ID represents peptide hit(s) obtained by NIH non-redundant database search and identified by their corresponding gene identifiers, as well as common names (in parenthesis).

Supplemental Table S2. The list of peptides identified in TAP-WPP2 LC/MS/MS analysis, corresponding to HSC70.

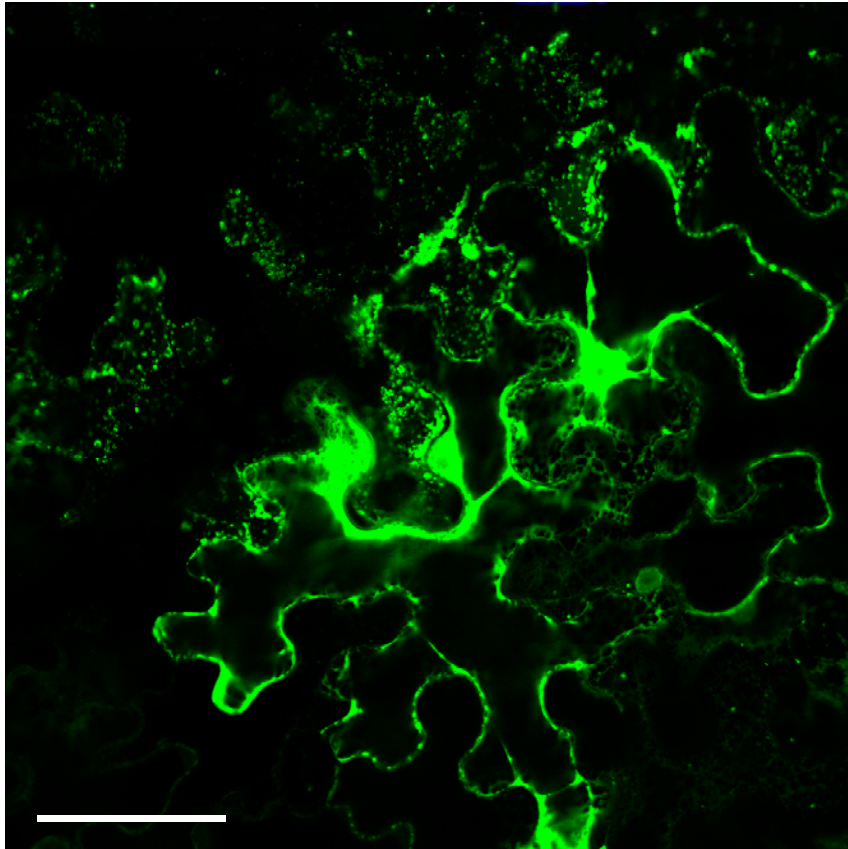
peptide	MH+	charge	XCorr score	Delta Cn score	Protein ID
KMYQGGEAGGPAAGGMDEDVPPSAGGAGPKI	2663.14	2	2.26	0.28	At3g09440 (HSC70-3)
KNQVAMNPINTVFDKR	1677.83	2	3.02	0.45	At3g09440 (HSC70-3)
KDAGVIAGLNVMRI	1215.65	2	1.99	0.12	At3g09440 (HSC70-3) At5g02500 (HSC70-1)
RIINEPTAAAIAYGLDKK	1659.90	2	4.02	0.62	At5g42020 (BiP) At1g56410 (HSP70T-1) At1g16030 (HSP70B) At3g12580 (HSP70) At5g28540 (BiP-1) At5g02490 (HSC70-2) At3g09440 (HSC70-3) At5g02500 (HSC70-1)
KEQVFSTYSDNQPGVLIQVYEGERA	2658.27	2	2.09	0.32	At3g09440 (HSC70-3) At5g02500 (HSC70-1)

Predicted mass (MH+) and charge values, as well as confidence parameters (Xcorr and Delta Cn) are indicated for each peptide. Protein ID represents peptide hit(s) obtained by NIH non-redundant database search and identified by their corresponding gene identifiers, as well as common names (in parenthesis).

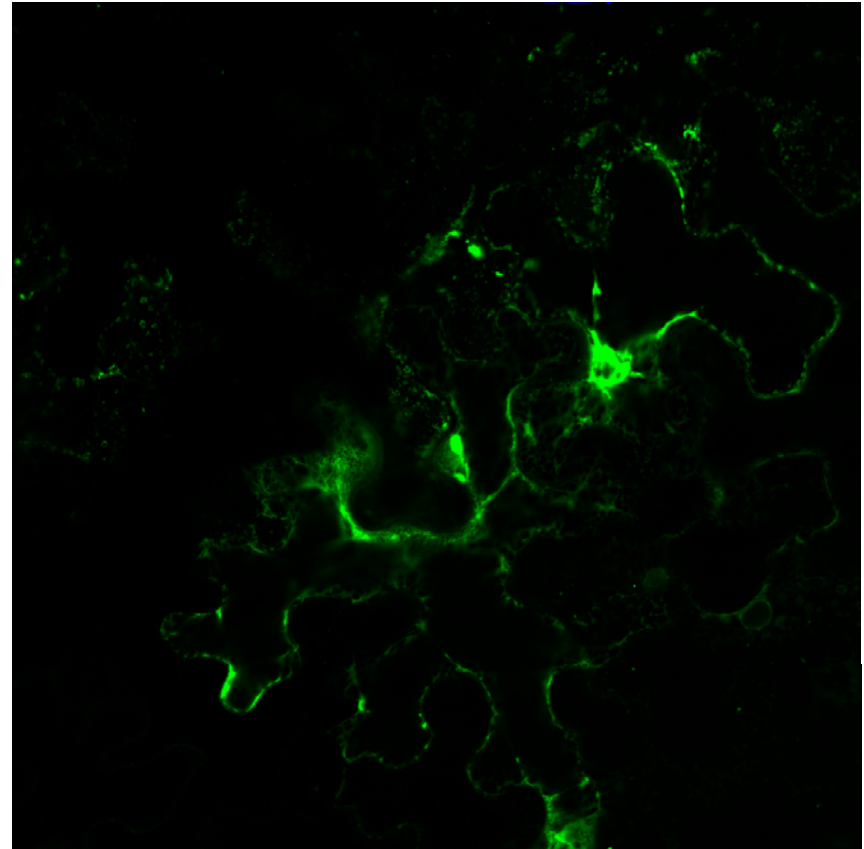


Supplemental Fig. S1. A. GFP-WIT1 aggregates in *N. benthamiana* leaves. GFP-WIT1 was agroinfiltrated in *N. benthamiana* leaves in the presence of p19. Final OD₆₀₀ used for infiltration was 0.5. B. GFP-WIT1 aggregation decreases with decreased OD₆₀₀ of the agroinfiltrated culture. GFP-WIT1 was agroinfiltrated in *N. benthamiana* leaves in the presence of p19. Final OD₆₀₀ used for infiltration is given below corresponding image. White arrows in B, nuclei. All scale bars: 10 μ m.

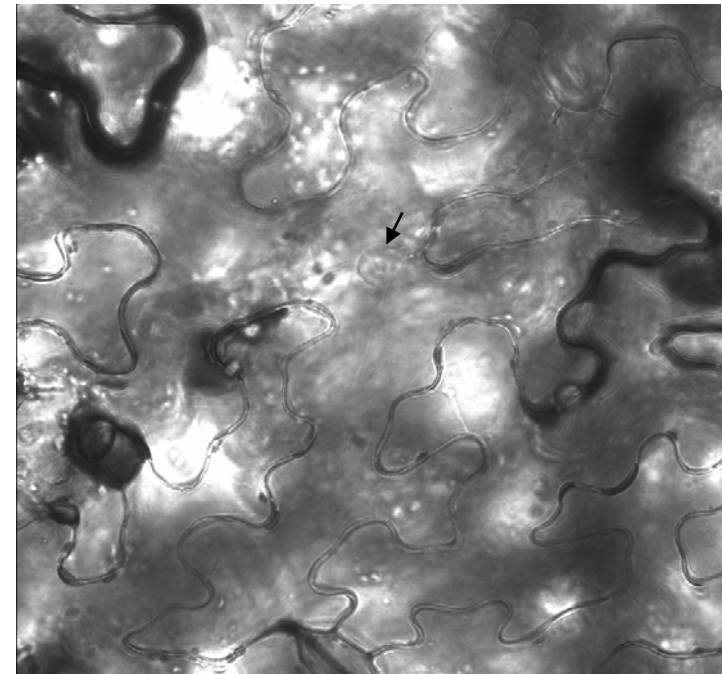
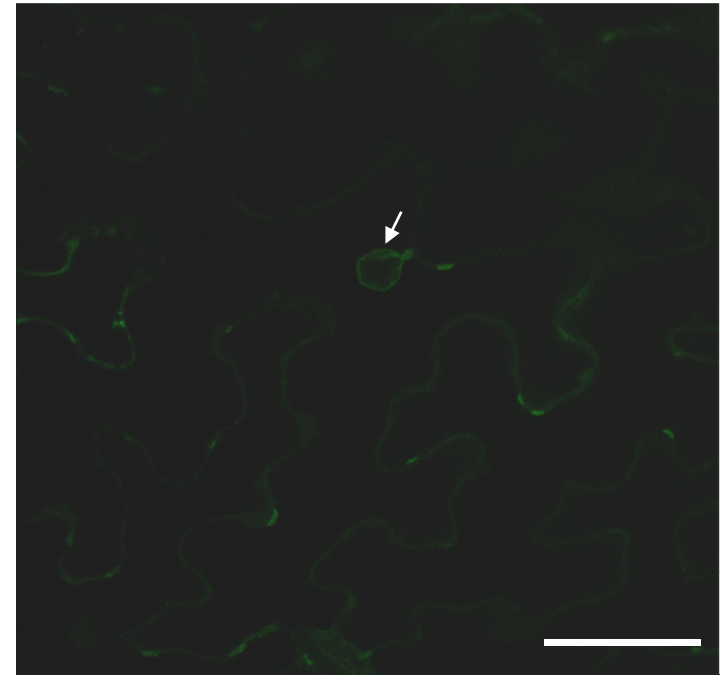
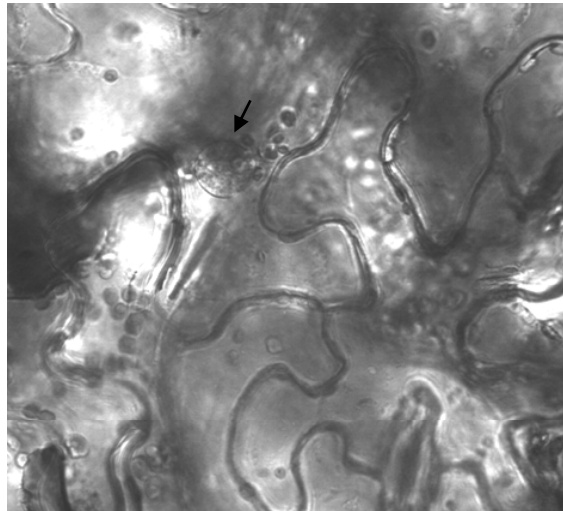
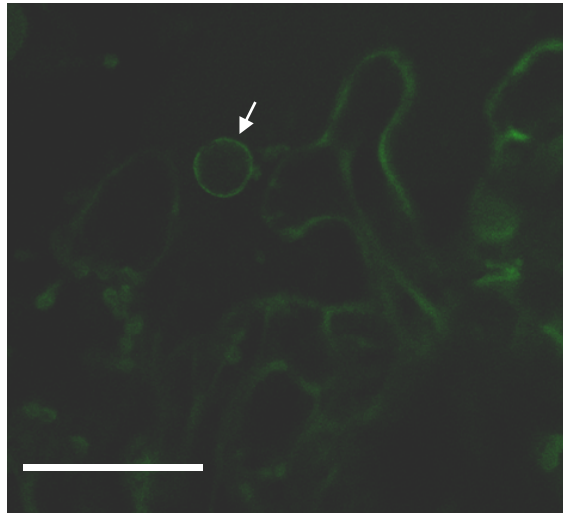
high



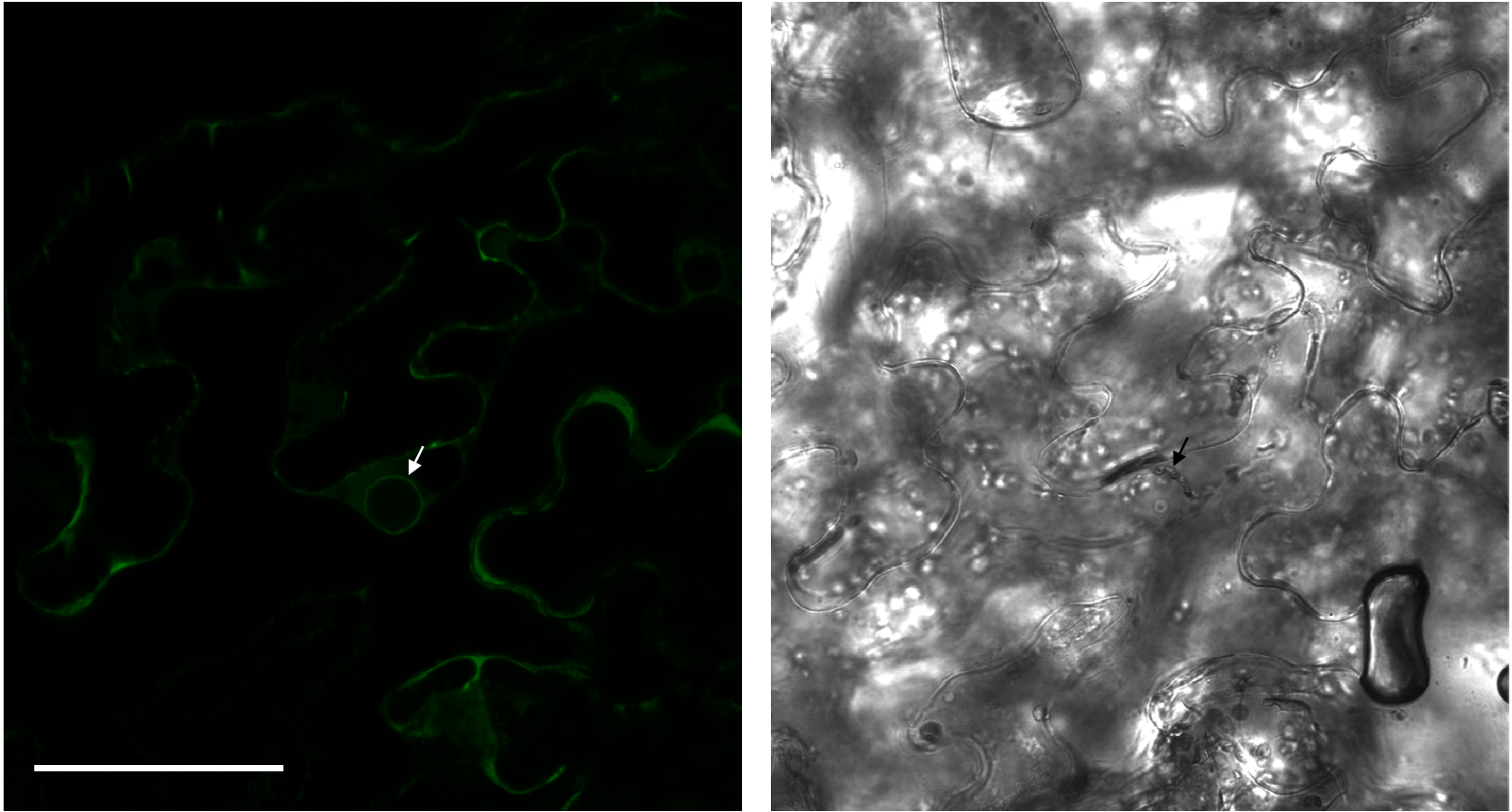
low



Supplemental Fig. S2. GFP-WIT1 aggregates do not form membrane whorls. GFP-WIT1 was agroinfiltrated in *N. benthamiana* leaves in the presence of p19. The images were taken at two different gain settings (high and low). Scale bar: 10 μm .

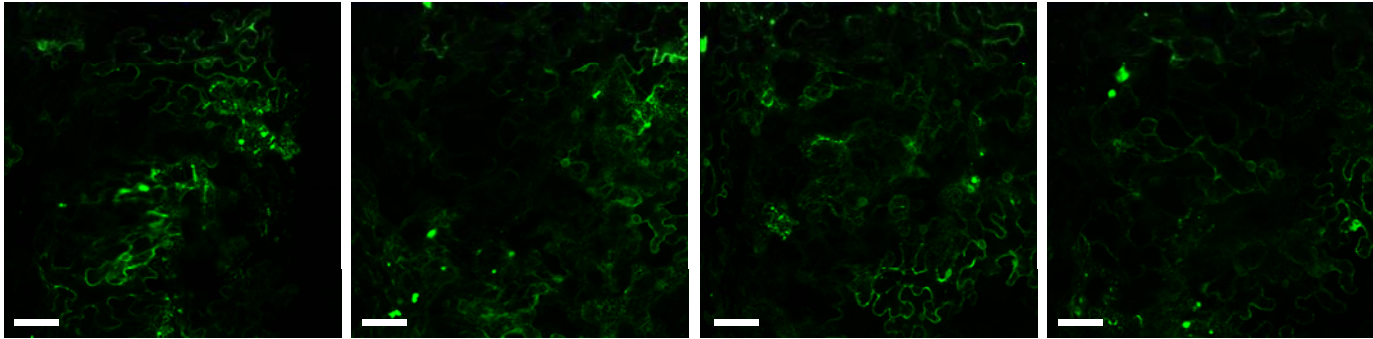


Supplemental Fig. S3. GFP-WIT1 is localized at the nuclear envelope in the absence of p19. GFP-WIT1 was agroinfiltrated in *N. benthamiana* leaves in the absence of p19. Bright field images are shown below two examples to indicate the position of the nucleus (white arrows in epifluorescence and black arrows in bright-field images). All scale bars: 10 μm .

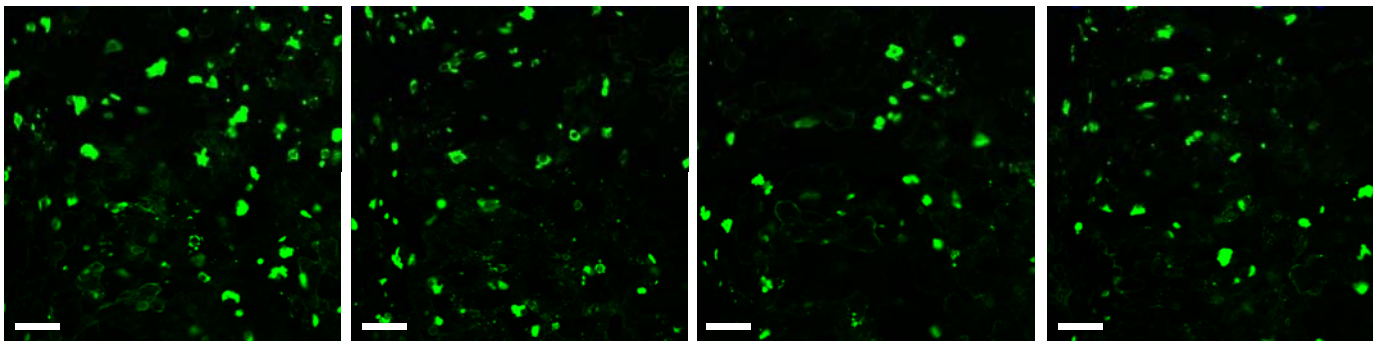


Supplemental Fig. S4. GFP-WIT1 is localized at the nuclear envelope when co-expressed with HA-WPP1. GFP-WIT1 was co-expressed in *N. benthamiana* leaves with HA-WPP1 in the presence of p19. Bright field image is shown to indicate the position of the nucleus (white arrow in epifluorescence and black arrow in bright-field image). Scale bar: 10 μm .

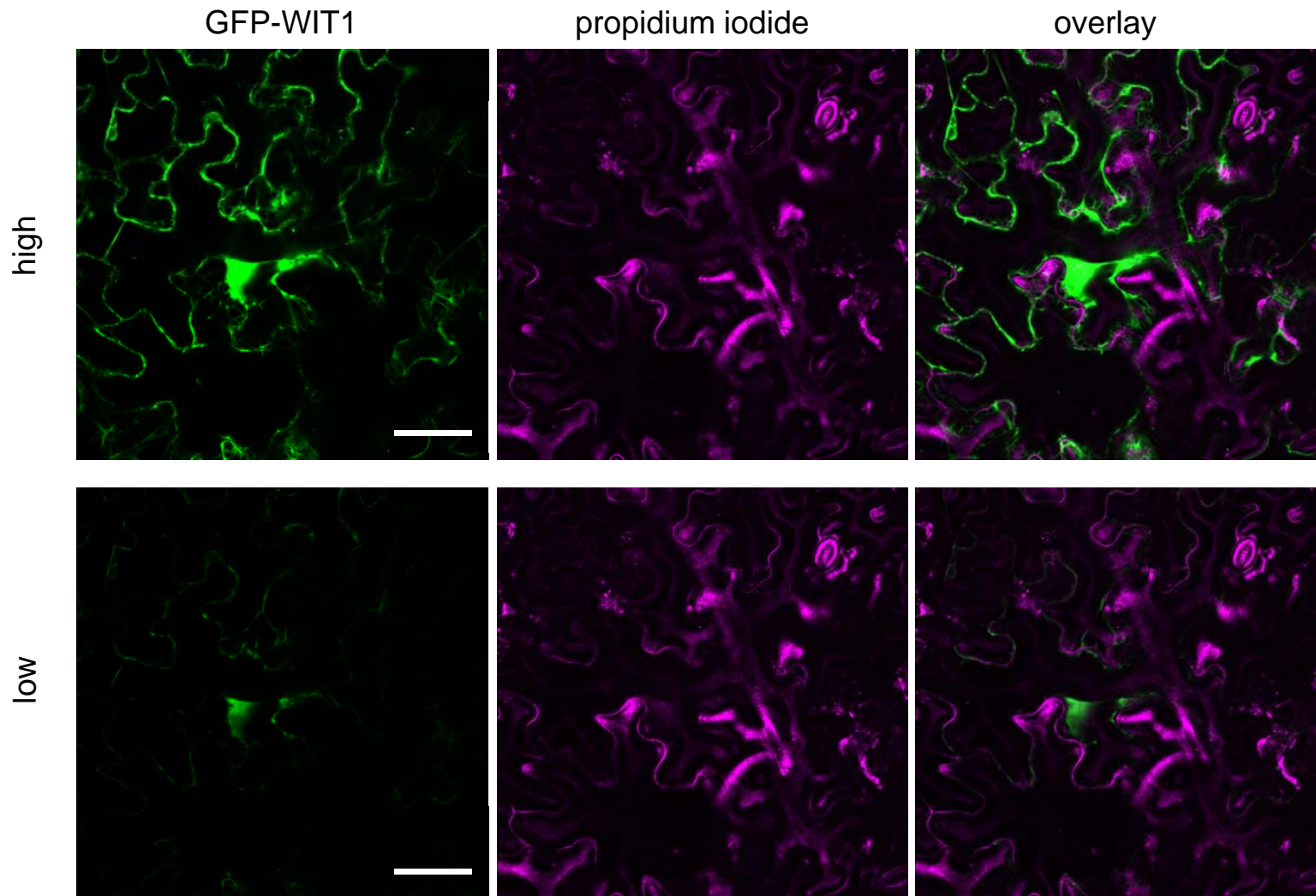
HA-HSC70-1 + GFP-WIT1



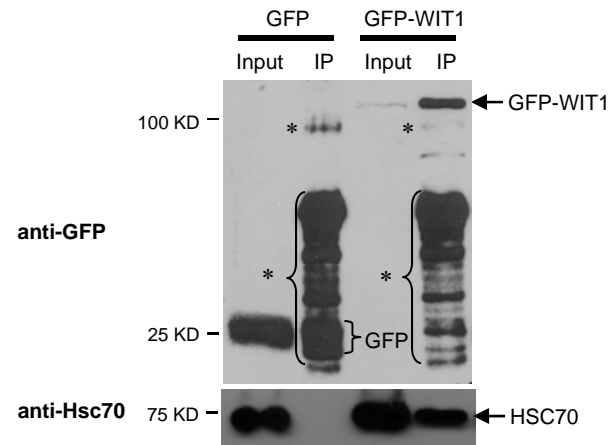
HA-HSC70-3 + GFP-WIT1



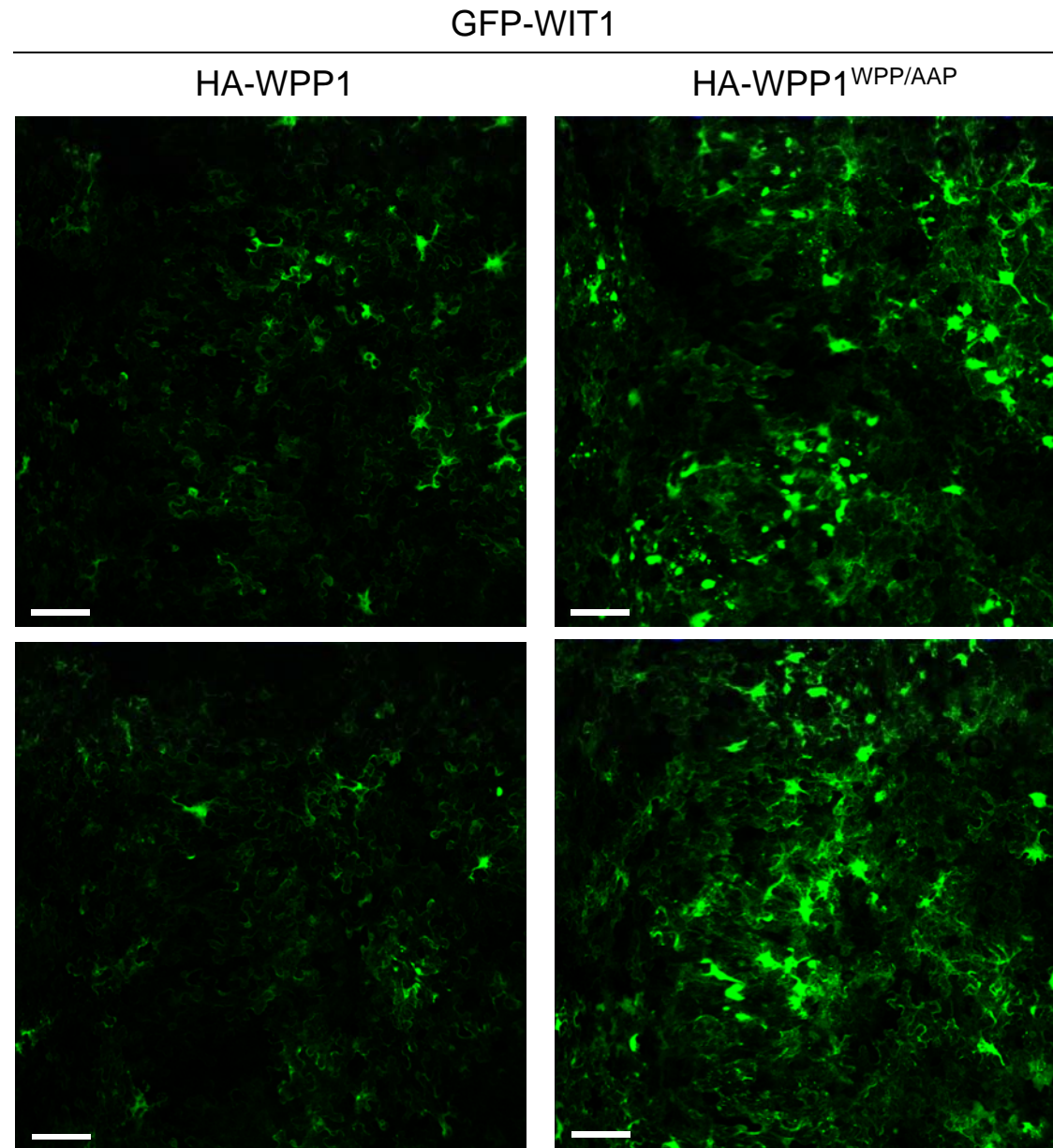
Supplemental Fig. S5. Unlike HSC70-3, HSC70-1 partially prevents GFP-WIT1 aggregation in *N. benthamiana*. GFP-WIT1 was co-expressed with one of the HA tagged constructs: HSC70-1 and HSC70-3 in *N. benthamiana* leaves by co-agroinfiltration in the presence of p19. All scale bars: 10 μ m.



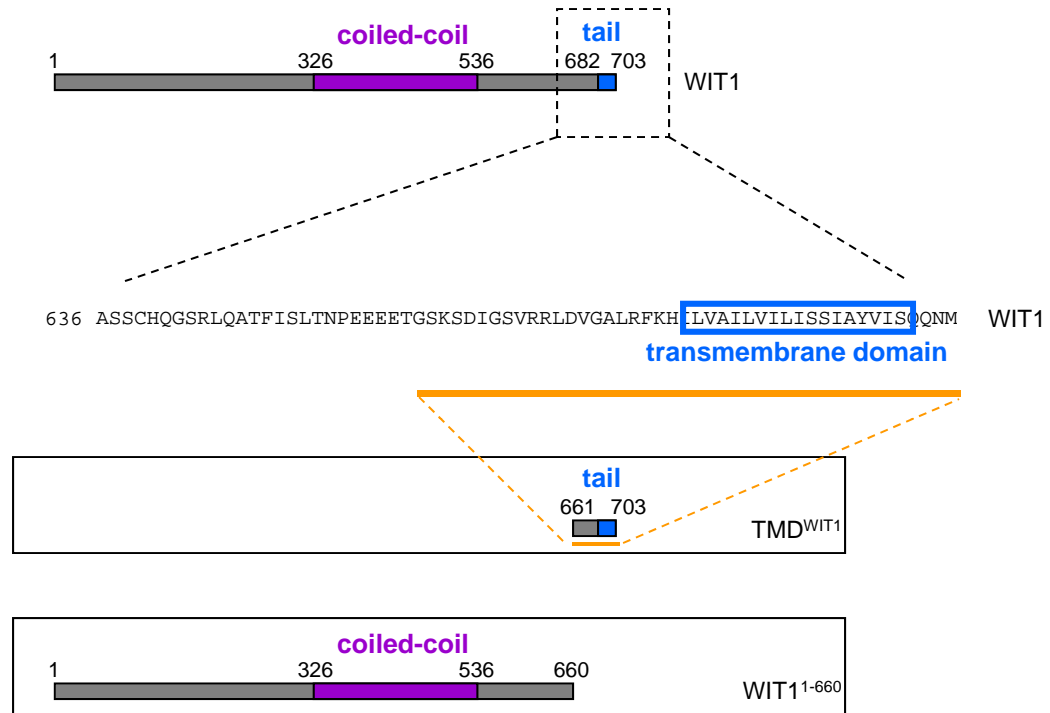
Supplemental Fig. S6. Cells that contain GFP-WIT1 aggregates are viable. GFP-WIT1 (green) was co-expressed in *N. benthamiana* leaves with HA-GUS in the presence of p19. Cell walls were counterstained with propidium iodide (magenta). The images were taken at two different gain settings (high and low) for better visualisation of cell boundary of the cell with GFP-WIT1 aggregate. Scale bar: 10 μm .



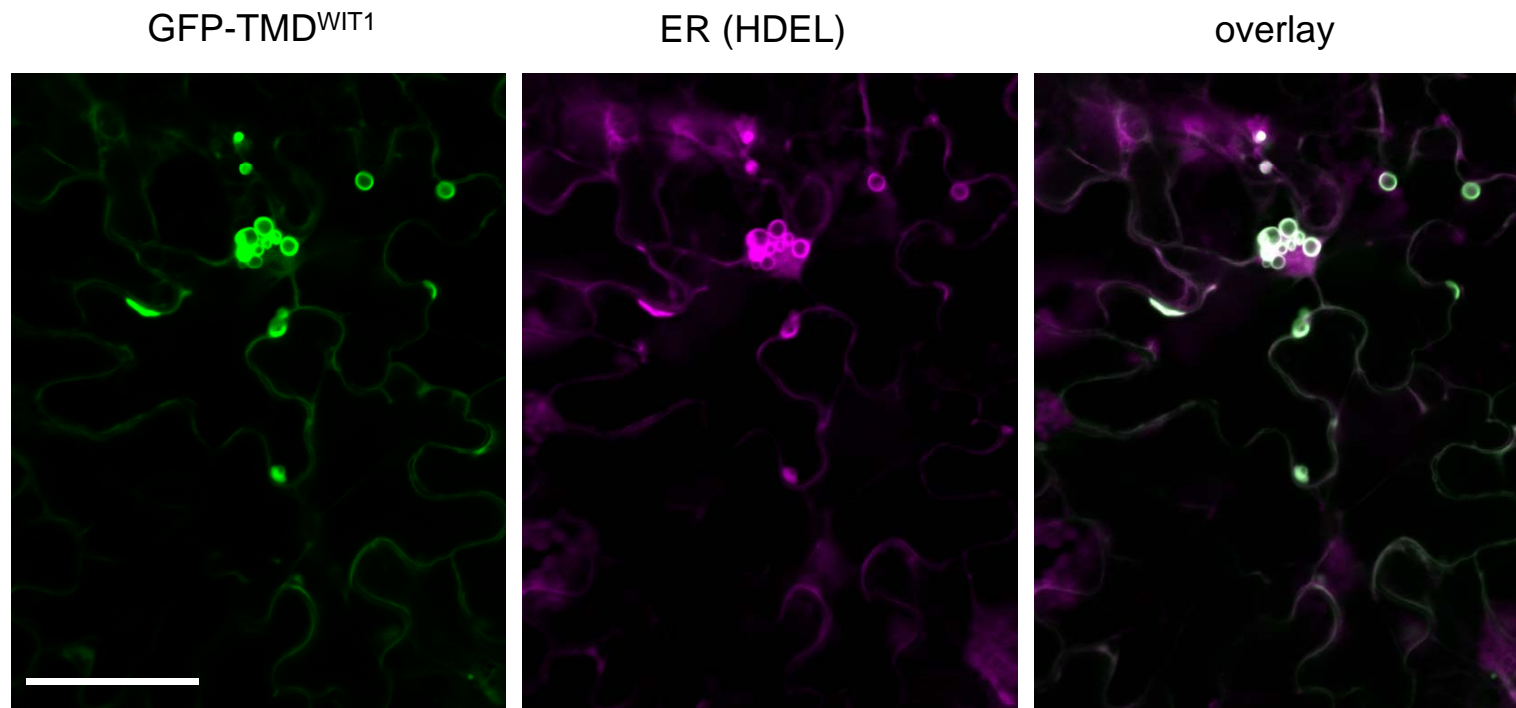
Supplemental Fig. S7. Samples immunoprecipitated from GFP and GFP-WIT1 Arabidopsis transgenic lines using the anti-GFP antibody, were probed with the anti-Hsc70 antibody. Non-specific signals coming from cross-reactivity of IgG with a secondary antibody are shown by asterisks. The positions of all proteins are depicted with arrows.



Supplemental Fig. S8. WPP1^{WPP/AAP} does not prevent GFP-WIT1 aggregation in *N. benthamiana*. GFP-WIT1 was co-expressed with either HA-WPP1 or HA-WPP1^{WPP/AAP} in *N. benthamiana* leaves by co-agroinfiltration in the presence of p19. All scale bars: 20 μ m.



Supplemental Fig. S9. Domain structure of WIT1 and WIT1 deletion constructs.



Supplemental Fig. S10. C-terminus of WIT1 co-localizes with the ER marker. GFP-TMD^{WIT1} (green) was co-expressed in *N. benthamiana* leaves with the ER marker (magenta) in the presence of p19. Scale bar: 10 μ m.